Partial wave analysis of $\pi\pi$ scattering below 2 GeV

V. Nazari[a]
P. Bydžovský[b], R. Kamiński[a]

[a]Institute of Nuclear Physics, Polish Academy of Sciences, Kraków, Poland
[b]Nuclear Physics Institute, ASCR, Řež/Prague, Czech Republic

14th International Workshop on Meson Production
Kraków, Poland

2-7 June 2016

Outline

1. Definition of the problem
2. Why it is so important?
3. How to solve it?
4. Method
5. Results of S and P waves
6. D and F wave amplitudes
7. Results of D and F waves
8. Conclusions

Definition of the problem

Lack of correct partial wave amplitudes for D and F waves in the $I^G J^{PC} = 0^+2^{++}$ and the 1^+3^{--} sectors to study the f_2 and ρ_3 mesons respectively.

The Main Problems:

- Lack of crossing symmetry condition.
- Unsuitable behavior of phase shift in vicinity of the $\pi\pi$ threshold.

Definition of the problem

Lack of correct partial wave amplitudes for D and F waves in the $I^G J^{PC} = 0^+2^{++}$ and the 1^+3^{--} sectors to study the f_2 and ρ_3 mesons respectively.

The Main Problems:

- Lack of crossing symmetry condition.
- Unsuitable behavior of phase shift in vicinity of the $\pi\pi$ threshold.

- Similar problems for S and P waves have been derived and presented in: Phys. Rev. D 83 (2011) 074004
- Further analysis presented a very precise determination for position of the σ pole in: Phys. Rev. Lett. 107 (2011) 072001
- Proof of the results by unitary multi-channel $\pi\pi$ scattering amplitudes: Phys. Rev. D 90, (2014) 116005

Definition of the problem

Lack of correct partial wave amplitudes for D and F waves in the $I^G J^{PC} = 0^+2^{++}$ and the 1^+3^{--} sectors to study the f_2 and ρ_3 mesons respectively.

The Main Problems:

- Lack of crossing symmetry condition.
- Unsuitable behavior of phase shift in vicinity of the $\pi\pi$ threshold.

- Similar problems for S and P waves have been derived and presented in: Phys. Rev. D 83 (2011) 074004
- Further analysis presented a very precise determination for position of the σ pole in: Phys. Rev. Lett. 107 (2011) 072001
- Proof of the results by unitary multi-channel $\pi\pi$ scattering amplitudes: Phys. Rev. D 90, (2014) 116005

Significances

- Old parameterizations are still used.

Significances

- Old parameterizations are still used.
- Specifying the dominant and ineffective states.

Significances

- Old parameterizations are still used.
- Specifying the dominant and ineffective states.
- Precise parameterizations of $\pi\pi$ amplitudes is crucial:
  - When high precision of the final state interactions is required. In analyses of the $\pi\pi$ final state interactions in the heavy mesons decays (e.g. B or $D \to M\pi\pi$ where M is K or π)
  - To describe spectrum of light mesons decaying into $\pi\pi$ pairs.

Significances

- Old parameterizations are still used.
- Specifying the dominant and ineffective states.
- Precise parameterizations of $\pi\pi$ amplitudes is crucial:
  - When high precision of the final state interactions is required. In analyses of the $\pi\pi$ final state interactions in the heavy mesons decays (e.g. B or $D \to M\pi\pi$ where M is K or π)
  - To describe spectrum of light mesons decaying into $\pi\pi$ pairs.
- Photoproduction of exotic mesons - The CLAS12 Detector at Jefferson Lab.

Significances

- Old parameterizations are still used.
- Specifying the dominant and ineffective states.
- Precise parameterizations of $\pi\pi$ amplitudes is crucial:
  - When high precision of the final state interactions is required. In analyses of the $\pi\pi$ final state interactions in the heavy mesons decays (e.g. B or $D \to M\pi\pi$ where M is K or π)
  - To describe spectrum of light mesons decaying into $\pi\pi$ pairs.
- Photoproduction of exotic mesons - The CLAS12 Detector at Jefferson Lab.

Structure of the amplitudes

- Resonance contributions of poles and zeros on the Riemann surface.
- The list of contributing resonant states for the D0 wave is according to the latest issue of PDG. $f_2(1270)$, $f_2(1430)$, $f_2(1525)$, $f_2(1640)$, $f_2(1810)$, $f_2(1910)$, $f_2(1950)$, $f_2(2010)$, $f_2(2150)$, $f_2(2300)$, $f_2(2340)$,$f_2(1565)$

Structure of the amplitudes

- Resonance contributions of poles and zeros on the Riemann surface.
- The list of contributing resonant states for the D0 wave is according to the latest issue of PDG. $f_2(1270)$, $f_2(1430)$, $f_2(1525)$, $f_2(1640)$, $f_2(1810)$, $f_2(1910)$, $f_2(1950)$, $f_2(2010)$, $f_2(2150)$, $f_2(2300)$, $f_2(2340)$,$f_2(1565)$
- For the F1 wave only one resonant state $\rho_3(1690)$ has been considered. $\rho_3(1990)$

Structure of the amplitudes

- Resonance contributions of poles and zeros on the Riemann surface.
- The list of contributing resonant states for the D0 wave is according to the latest issue of PDG. $f_2(1270)$, $f_2(1430)$, $f_2(1525)$, $f_2(1640)$, $f_2(1810)$, $f_2(1910)$, $f_2(1950)$, $f_2(2010)$, $f_2(2150)$, $f_2(2300)$, $f_2(2340)$,$f_2(1565)$
- For the F1 wave only one resonant state $\rho_3(1690)$ has been considered. $\rho_3(1990)$
- Channels have been considered for D wave: $\pi\pi$, $2\pi 2\pi$, $K\bar{K}$, $\eta\eta$.

Structure of the amplitudes

- Resonance contributions of poles and zeros on the Riemann surface.
- The list of contributing resonant states for the D0 wave is according to the latest issue of PDG. $f_2(1270)$, $f_2(1430)$, $f_2(1525)$, $f_2(1640)$, $f_2(1810)$, $f_2(1910)$, $f_2(1950)$, $f_2(2010)$, $f_2(2150)$, $f_2(2300)$, $f_2(2340)$, $f_2(1565)$
- For the F1 wave only one resonant state $\rho_3(1690)$ has been considered. $\rho_3(1990)$
- Channels have been considered for D wave: $\pi\pi$, $2\pi 2\pi$, $K\bar{K}$, $\eta\eta$.
- Channels have been considered for F wave: $\pi\pi$, $2\pi 2\pi$, $\omega\pi$, $K\bar{K}$.

Structure of the amplitudes

- Resonance contributions of poles and zeros on the Riemann surface.
- The list of contributing resonant states for the D0 wave is according to the latest issue of PDG. $f_2(1270)$, $f_2(1430)$, $f_2(1525)$, $f_2(1640)$, $f_2(1810)$, $f_2(1910)$, $f_2(1950)$, $f_2(2010)$, $f_2(2150)$, $f_2(2300)$, $f_2(2340)$,$f_2(1565)$
- For the F1 wave only one resonant state $\rho_3(1690)$ has been considered. $\rho_3(1990)$
- Channels have been considered for D wave: $\pi\pi$, $2\pi 2\pi$, $K\bar{K}$, $\eta\eta$.
- Channels have been considered for F wave: $\pi\pi$, $2\pi 2\pi$, $\omega\pi$, $K\bar{K}$.
- Utilizing formulas for analytical continuations of the S-matrix elements.

Structure of the amplitudes

- Resonance contributions of poles and zeros on the Riemann surface.
- The list of contributing resonant states for the D0 wave is according to the latest issue of PDG. $f_2(1270)$, $f_2(1430)$, $f_2(1525)$, $f_2(1640)$, $f_2(1810)$, $f_2(1910)$, $f_2(1950)$, $f_2(2010)$, $f_2(2150)$, $f_2(2300)$, $f_2(2340)$,$f_2(1565)$
- For the F1 wave only one resonant state $\rho_3(1690)$ has been considered. $\rho_3(1990)$
- Channels have been considered for D wave: $\pi\pi$, $2\pi 2\pi$, $K\bar{K}$, $\eta\eta$.
- Channels have been considered for F wave: $\pi\pi$, $2\pi 2\pi$, $\omega\pi$, $K\bar{K}$.
- Utilizing formulas for analytical continuations of the S-matrix elements.
- The matrix elements S_{ij} of the N -channel S matrix $(i, j = 1, 2, ...N)$ are expressed via the Jost matrix determinant, $d(k_1, k_2, ...k_N)$ (k_i are the channel momenta), using the Le Couteur-Newton relations.

Structure of the amplitudes

- Resonance contributions of poles and zeros on the Riemann surface.
- The list of contributing resonant states for the D0 wave is according to the latest issue of PDG. $f_2(1270)$, $f_2(1430)$, $f_2(1525)$, $f_2(1640)$, $f_2(1810)$, $f_2(1910)$, $f_2(1950)$, $f_2(2010)$, $f_2(2150)$, $f_2(2300)$, $f_2(2340)$,$f_2(1565)$
- For the F1 wave only one resonant state $\rho_3(1690)$ has been considered. $\rho_3(1990)$
- Channels have been considered for D wave: $\pi\pi$, $2\pi 2\pi$, $K\bar{K}$, $\eta\eta$.
- Channels have been considered for F wave: $\pi\pi$, $2\pi 2\pi$, $\omega\pi$, $K\bar{K}$.
- Utilizing formulas for analytical continuations of the S-matrix elements.
- The matrix elements S_{ij} of the N -channel S matrix $(i, j = 1, 2, ...N)$ are expressed via the Jost matrix determinant, $d(k_1, k_2, ...k_N)$ (k_i are the channel momenta), using the Le Couteur-Newton relations.

Structure of the amplitudes

- The Jost determinant is considered in a separable form $d = d_{bgr} d_{res}$.
  - The resonance part is described by the multi-channel Breit-Wigner form:

$$d_{res}(s) = \prod_r \left[M_r^2 - s - i \sum_{i=1}^{N} \rho_{ri}^{2J+1} R_{ri} f_{ri}^2 \right] \tag{1}$$

$$R_{ri} = \frac{9 + \frac{3}{4}\left(\sqrt{M_r^2 - s_i}\; r_{ri}\right)^2 + \frac{1}{16}\left(\sqrt{M_r^2 - s_i}\; r_{ri}\right)^4}{9 + \frac{3}{4}\left(\sqrt{s - s_i}\; r_{ri}\right)^2 + \frac{1}{16}\left(\sqrt{s - s_i}\; r_{ri}\right)^4} \tag{2}$$

Structure of the amplitudes

- The Jost determinant is considered in a separable form $d = d_{bgr} d_{res}$.
  - The resonance part is described by the multi-channel Breit-Wigner form:

$$d_{res}(s) = \prod_r \left[M_r^2 - s - i \sum_{i=1}^{N} \rho_{ri}^{2J+1} R_{ri} f_{ri}^2 \right] \quad (1)$$

$$R_{ri} = \frac{9 + \frac{3}{4}\left(\sqrt{M_r^2 - s_i}\; r_{ri}\right)^2 + \frac{1}{16}\left(\sqrt{M_r^2 - s_i}\; r_{ri}\right)^4}{9 + \frac{3}{4}\left(\sqrt{s - s_i}\; r_{ri}\right)^2 + \frac{1}{16}\left(\sqrt{s - s_i}\; r_{ri}\right)^4} \quad (2)$$

  - The background part d_{bgr}:which represents mainly an influence of neglected channels and resonances.

    For D wave:

$$d_{bgr} = \exp\left[-i \sum_{i=1}^{4} \left(\sqrt{\frac{s - s_i}{s}} \right)^5 (a_i + i b_i) \right] \quad (3)$$

For F wave:

$$d_{bgr} = \exp\left[-i \left(\sqrt{\frac{s - s_i}{s}} \right)^{7/2} \left(a_\alpha + \frac{s - s_i}{s_i} a_\beta + \left(\frac{s - s_i}{s_i} \right)^2 a_\gamma \right) \right] \quad (4)$$

Structure of the amplitudes

- The Jost determinant is considered in a separable form $d = d_{bgr} d_{res}$.
  - The resonance part is described by the multi-channel Breit-Wigner form:

$$d_{res}(s) = \prod_r \left[M_r^2 - s - i \sum_{i=1}^{N} \rho_{ri}^{2J+1} R_{ri} f_{ri}^2 \right] \tag{1}$$

$$R_{ri} = \frac{9 + \frac{3}{4}\left(\sqrt{M_r^2 - s_i}\ r_{ri}\right)^2 + \frac{1}{16}\left(\sqrt{M_r^2 - s_i}\ r_{ri}\right)^4}{9 + \frac{3}{4}\left(\sqrt{s - s_i}\ r_{ri}\right)^2 + \frac{1}{16}\left(\sqrt{s - s_i}\ r_{ri}\right)^4} \tag{2}$$

  - The background part d_{bgr}:which represents mainly an influence of neglected channels and resonances.
    For D wave:

$$d_{bgr} = \exp\left[-i \sum_{i=1}^{4} \left(\sqrt{\frac{s - s_i}{s}} \right)^5 (a_i + i b_i) \right] \tag{3}$$

For F wave:

$$d_{bgr} = \exp\left[-i \left(\sqrt{\frac{s - s_i}{s}} \right)^{7/2} \left(a_\alpha + \frac{s - s_i}{s_i} a_\beta + \left(\frac{s - s_i}{s_i} \right)^2 a_\gamma \right) \right] \tag{4}$$

Dispersion relations with imposed crossing symmetry

Crossing Symmetry:

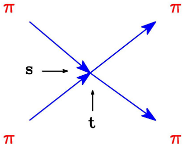

$\longrightarrow \quad \overrightarrow{T_s}(\mathrm{s,t})=\hat{C}_{st}\,\overrightarrow{T_t}(\mathrm{t,s})$

Once-subtracted Dispersion Relations:

$$\boxed{\mathrm{Re}f_\ell^I(s)^{out} = \sum_{I'=0}^{2} C_{st}^{II'}\, a_0^{I'} + \sum_{I'=0}^{2}\sum_{\ell'=0}^{3}\int_{4m_\pi^2}^{S_{max}} ds'\, K_{\ell\ell'}^{II'}(s,s')\,\mathrm{Im}f_{\ell'}^{I'}(s')^{in} + d_\ell^I(s),}$$

"Subtracting term" **"Kernel term"** **"Driving term"**

$a_0^{I'}$ is Subtracting constant $= \overrightarrow{T_s}\ (s = 4m_\pi^2, t = 0)$

Dispersion relations with imposed crossing symmetry

Crossing Symmetry:

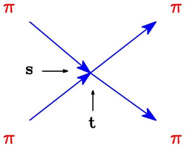

$$\longrightarrow \quad \vec{\boldsymbol{T}}_{\boldsymbol{s}}(\mathrm{s,t}) = \hat{\boldsymbol{C}}_{st}\, \vec{\boldsymbol{T}}_{\boldsymbol{t}}(\mathrm{t,s})$$

Once-subtracted Dispersion Relations:

$$\boxed{\mathrm{Re} f_\ell^I(s)^{out} = \sum_{I'=0}^{2} C_{st}^{II'}\, a_0^{I'} + \sum_{I'=0}^{2}\sum_{\ell'=0}^{3}\int_{4m_\pi^2}^{S_{max}} ds' K_{\ell\ell'}^{II'}(s,s')\mathrm{Im} f_{\ell'}^{I'}(s')^{in} + d_\ell^I(s),}$$

"Subtracting term" **"Kernel term"** **"Driving term"**

$a_0^{I'}$ is Subtracting constant $= \vec{\boldsymbol{T}}_{\boldsymbol{s}}\ (s = 4m_\pi^2, t = 0)$

$$\mathrm{Re} f_\ell^I(s)^{out} - \mathrm{Re} f_\ell^I(s)^{in} \longrightarrow 0$$

Dispersion relations with imposed crossing symmetry

Crossing Symmetry:

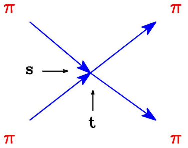

$\longrightarrow \quad \overrightarrow{\boldsymbol{T}}_{\boldsymbol{s}}(\mathrm{s,t}) = \hat{\boldsymbol{C}}_{st}\, \overrightarrow{\boldsymbol{T}}_{\boldsymbol{t}}(\mathrm{t,s})$

Once-subtracted Dispersion Relations:

$$\boxed{\mathrm{Re} f_\ell^I(s)^{out} = \sum_{I'=0}^{2} C_{st}^{II'} a_0^{I'} + \sum_{I'=0}^{2} \sum_{\ell'=0}^{3} \int_{4m_\pi^2}^{S_{max}} ds' K_{\ell\ell'}^{II'}(s,s') \mathrm{Im} f_{\ell'}^{I'}(s')^{in} + d_\ell^I(s),}$$

"Subtracting term" **"Kernel term"** **"Driving term"**

$a_0^{I'}$ is Subtracting constant $= \overrightarrow{\boldsymbol{T}}_{\boldsymbol{s}}\ (s = 4m_\pi^2, t = 0)$

$$\mathrm{Re} f_\ell^I(s)^{out} - \mathrm{Re} f_\ell^I(s)^{in} \longrightarrow 0$$

S and P wave amplitudes

- New amplitudes fulfilled crossing symmetry very well.

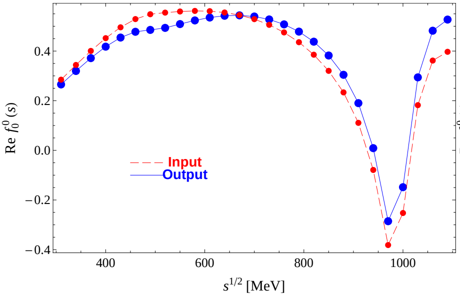

(a) $\mathrm{Re}f_0^0(s)^{IN}$ and $\mathrm{Re}f_0^0(s)^{OUT}$ amplitude before fitting.

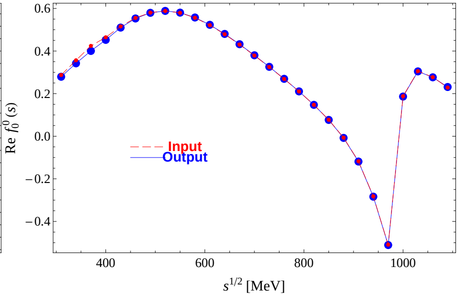

(b) $\mathrm{Re}f_0^0(s)^{IN}$ and $\mathrm{Re}f_0^0(s)^{OUT}$ amplitude after fitting.

S and P wave amplitudes

- New amplitudes fulfilled crossing symmetry very well.

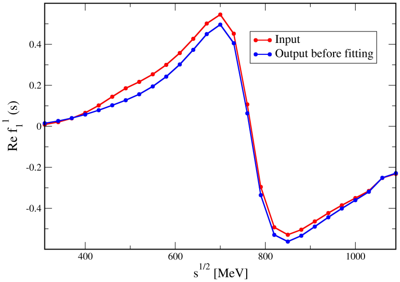

(c) $\mathrm{Re}f_1^1(s)^{IN}$ and $\mathrm{Re}f_1^1(s)^{OUT}$ amplitude before fitting.

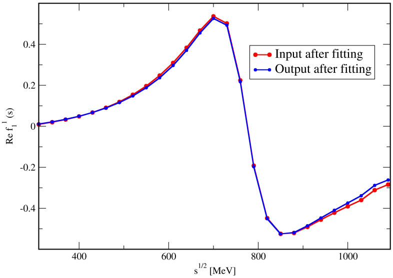

(d) $\mathrm{Re}f_1^1(s)^{IN}$ and $\mathrm{Re}f_1^1(s)^{OUT}$ amplitude after fitting.

S and P wave amplitudes

- New S and P wave amplitudes very well describe the experimental data.

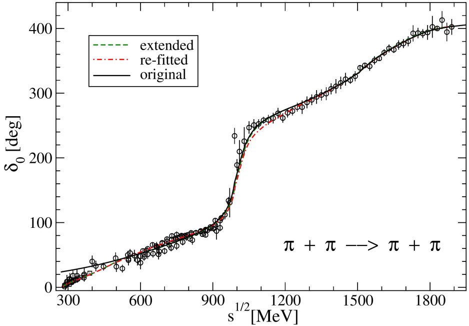

(e) Phase shift from threshold to 2 GeV

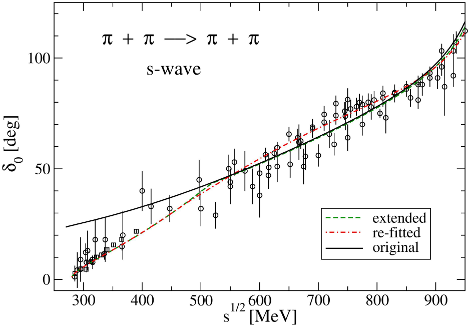

(f) Phase shift from threshold to 1 GeV

S and P wave amplitudes

- Shift of the σ pole. $617 - i\,554$ MeV $449^{+14}_{-14} - i289^{+14}_{-14}$ MeV
  - * Result based on ChPT and Roy-like equations $441^{+16}_{-8} - i272^{+9}_{-13}$ MeV
  - * Result based on GKPY equations $445^{+25}_{-25} - i278^{+22}_{-18}$ MeV

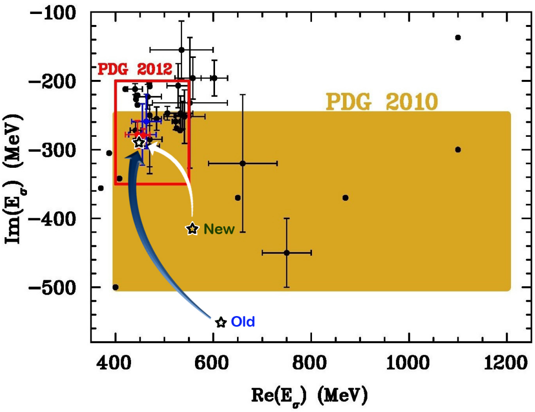

Figure : Shift of the σ pole.

Improving the paremeters for S and P waves

To improve agreement of the amplitudes with the CS the new amplitudes have been fitted to DR and to the data.
The total χ^2 was composed of five parts:

$$\chi^2 = \sum_{l=1}^{2} \chi^2_{Data}(\ell) + \sum_{j=1}^{3} \chi^2_{DR}(j) \tag{5}$$

where $j = 1, 2, 3$ itemizes the $S0$, $P1$ and $S2$ partial waves, respectively.
Corresponding $\chi^2_{Data}(j)$ and $\chi^2_{DR}(j)$ are expressed by

$$\chi^2_{Data}(j) = \sum_{i=1}^{N_\delta^j} \frac{(\delta_i^{exp} - \delta_i^{th})^2}{(\Delta\delta_i^{exp})^2} + \sum_{i=1}^{N_\eta^j} \frac{(\eta_i^{exp} - \eta_i^{th})^2}{(\Delta\eta_i^{exp})^2} \tag{6}$$

and

$$\chi^2_{DR}(j) = \sum_{i=1}^{N_{DR}} \left(\frac{\mathrm{Re} f_\ell^I(s_i)^{out} - \mathrm{Re} f_\ell^I(s_i)^{in}}{\Delta_{DR}} \right)^2 \tag{7}$$

Improving the paremeters for S and P waves

To improve agreement of the amplitudes with the CS the new amplitudes have been fitted to DR and to the data.
The total χ^2 was composed of five parts:

$$\chi^2 = \sum_{l=1}^{2} \chi^2_{Data}(\ell) + \sum_{j=1}^{3} \chi^2_{DR}(j) \quad (5)$$

where $j = 1, 2, 3$ itemizes the $S0$, $P1$ and $S2$ partial waves, respectively.
Corresponding $\chi^2_{Data}(j)$ and $\chi^2_{DR}(j)$ are expressed by

$$\chi^2_{Data}(j) = \sum_{i=1}^{N^j_\delta} \frac{(\delta_i^{exp} - \delta_i^{th})^2}{(\Delta\delta_i^{exp})^2} + \sum_{i=1}^{N^j_\eta} \frac{(\eta_i^{exp} - \eta_i^{th})^2}{(\Delta\eta_i^{exp})^2} \quad (6)$$

and

$$\chi^2_{DR}(j) = \sum_{i=1}^{N_{DR}} \left(\frac{\mathrm{Re} f^I_\ell(s_i)^{out} - \mathrm{Re} f^I_\ell(s_i)^{in}}{\Delta_{DR}} \right)^2 \quad (7)$$

S and P wave amplitudes

	χ^2	$\chi^2_{Data}(S0)$	$\chi^2_{Data}(P1)$	χ^2_{DR}
extended	1122.5	339.4	305.1	478.0
re-fitted	605.5	269.0	300.9	35.6

Table : Values of the χ^2 for the extended (before fitting) and re-fitted (after fitting) amplitudes.

Improving the paremeters for 0^+2^{++} and 1^+3^{--} sectors

To improve agreement of the amplitudes with the CS the new amplitudes have been fitted to DR and to the data.
The total χ^2 was composed of ten parts:

$$\chi^2 = \sum_{j=0}^{3} \chi^2_{Data}(j) + \sum_{j=0}^{3} \chi^2_{DR}(j) \tag{8}$$

where $j = 0, ..., 3$ itemizes all partial waves, respectively. Corresponding $\chi^2_{Data}(j)$ and $\chi^2_{DR}(j)$ are expressed by

$$\chi^2_{Data}(j) = \sum_{i=1}^{N^j_\delta} \frac{(\delta_i^{exp} - \delta_i^{th})^2}{(\Delta\delta_i^{exp})^2} + \sum_{i=1}^{N^j_\eta} \frac{(\eta_i^{exp} - \eta_i^{th})^2}{(\Delta\eta_i^{exp})^2} \tag{9}$$

and

$$\chi^2_{DR}(j) = \sum_{i=1}^{N_{DR}} \left(\frac{\mathrm{Re} f_\ell^I(s_i)^{out} - \mathrm{Re} f_\ell^I(s_i)^{in}}{\Delta_{DR}} \right)^2 \tag{10}$$

Improving the paremeters for 0^+2^{++} and 1^+3^{--} sectors

To improve agreement of the amplitudes with the CS the new amplitudes have been fitted to DR and to the data.
The total χ^2 was composed of ten parts:

$$\chi^2 = \sum_{j=0}^{3} \chi^2_{Data}(j) + \sum_{j=0}^{3} \chi^2_{DR}(j) \tag{8}$$

where $j = 0, ..., 3$ itemizes all partial waves, respectively. Corresponding $\chi^2_{Data}(j)$ and $\chi^2_{DR}(j)$ are expressed by

$$\chi^2_{Data}(j) = \sum_{i=1}^{N^j_\delta} \frac{(\delta_i^{exp} - \delta_i^{th})^2}{(\Delta\delta_i^{exp})^2} + \sum_{i=1}^{N^j_\eta} \frac{(\eta_i^{exp} - \eta_i^{th})^2}{(\Delta\eta_i^{exp})^2} \tag{9}$$

and

$$\chi^2_{DR}(j) = \sum_{i=1}^{N_{DR}} \left(\frac{\mathrm{Re} f_\ell^I(s_i)^{out} - \mathrm{Re} f_\ell^I(s_i)^{in}}{\Delta_{DR}} \right)^2 \tag{10}$$

Results of D and F waves

- New the amplitudes for D and F waves very well describe the experimental data.

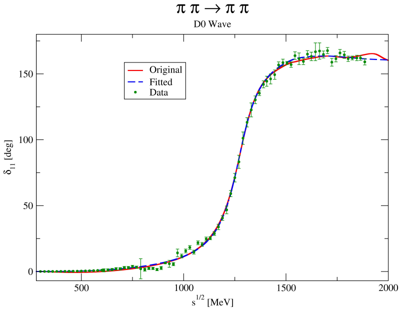

(a) Phase shift from threshold to 2 GeV

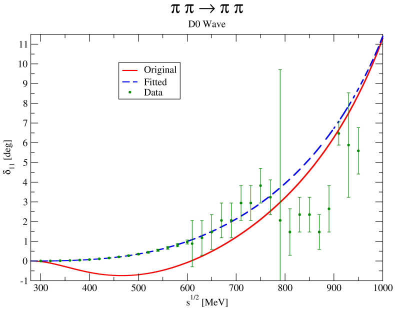

(b) Phase shift from threshold to 1 GeV

Results of D and F waves

- New the amplitudes for D and F waves very well describe the experimental data.

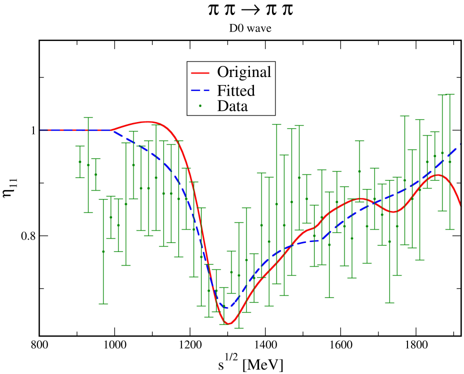

Figure : Inelasticity of the $D0$ wave.

Results of D and F waves

- New the amplitudes for D and F waves very well describe the experimental data.

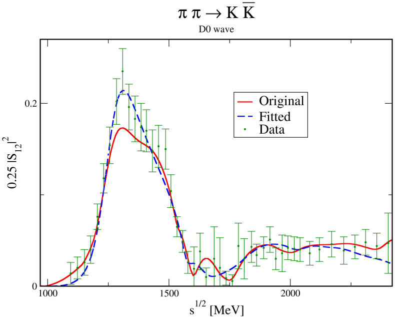

(a) Inelasticity for $K\bar{K}$ channel

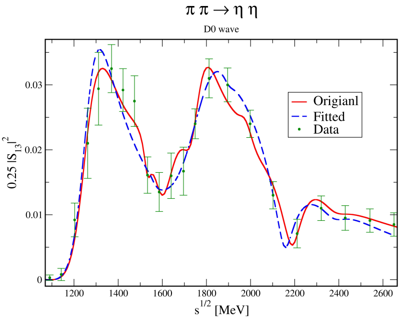

(b) Inelasticity for $\eta\eta$ channel

Results of D and F waves

- New the amplitudes for D and F waves very well describe the experimental data.

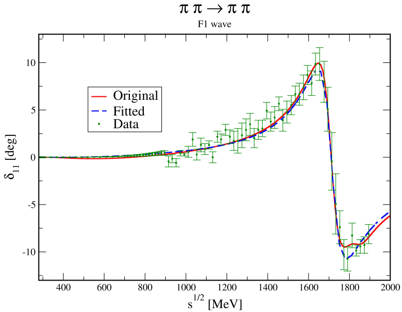

(c) Phase shift from threshold to 2 GeV

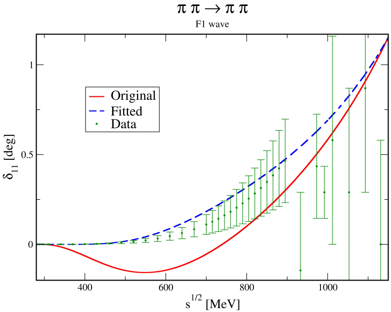

(d) Phase shift from threshold to 1 GeV

Results of D and F waves

- New the amplitudes for D and F waves very well describe the experimental data.

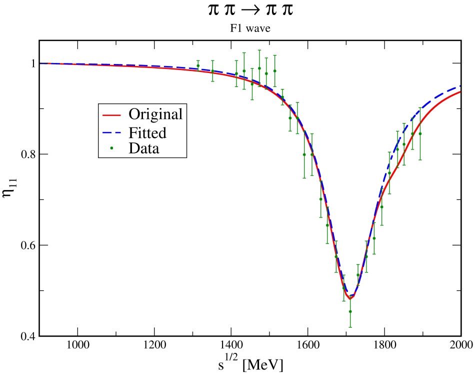

Figure : Inelasticity of the $F1$ wave.

Conclusions

- Achieved the new amplitudes for D and F waves which very well describe the experimental data.
- New amplitudes fulfilled crossing symmetry very well.
- The dominant and the ineffective resonance states of 0^+2^{++} sector:

States:	$f_2(1270)$	$f_2(1430)$	$f_2(1525)$	$f_2(1640)$	$f_2(1810)$
$f_2(1910)$	$f_2(1950)$	$f_2(2010)$	$f_2(2150)$	$f_2(2300)$	$f_2(2340)$

- The dominant and the ineffective resonance states of 1^+3^{--} sector:

States:	$\rho_3(1690)$	$\rho_3(1990)$

- Values of the χ^2 for re-fitted (after fitting) amplitudes:
  n.d.f= 891

$\chi^2_{Data}(S)$	$\chi^2_{Data}(P)$	$\chi^2_{Data}(D)$	$\chi^2_{Data}(F)$	χ^2_{DR}	χ^2	$\chi^2/n.d.f$
291.62	300.07	221.88	136.49	132.16	1082.22	1.21

Table : Values of the χ^2 using all new wave amplitudes after fitting.

Thank you for your attention.

Conclusions

Fit No.		χ^2
1	All stated are included	346.6
	Omitted States	
2	$f_2(1270)$	5426.0
3	$f_2(1430)$	345.1
4	$f_2(1525)$	354.0
5	$f_2(1640)$	395.0
6	$f_2(1810)$	338.2
7	$f_2(1910)$	347.1
8	$f_2(1950)$	346.5
9	$f_2(2010)$	346.2
10	$f_2(2150)$	373.0
11	$f_2(2300)$	347.8
12	$f_2(2340)$	346.5
13	$f_2(1430)$ $f_2(1810)$	340.1
14	$f_2(1950)$ $f_2(2010)$ $f_2(2340)$	346.2

Table : Values of χ^2 after fitting when some specific resonance states are omitted in the D wave.